Compressive large deformation viscoelastic behaviour of a polycarbonate

G. Titomanlio and G. Rizzo
Istituto di Ingegneria Chimica, Università di Palermo, Italy
(Received 4 November 1978; revised 28 February 1979)

The effect of deformation level and loading rate on compression creep and stress–relaxation behaviour of a polycarbonate has been studied. The possibility of obtaining master curves has been examined throughout. Satisfactory results were obtained for the stress–relaxation data by considering only the relaxable part of stress and by using a time shift factor proportional to both the inverse of deformation rate just prior to the test and the strain. The same shift factor allowed us to obtain a single master curve for the creep data.

INTRODUCTION

The viscoelastic behaviour of solid polymers for sufficiently small values of stress and/or strain is described by linear viscoelasticity theory. At larger strains, the viscoelastic behaviour is much more complex and only limited aspects of it have been described by means of relatively simple equations. One of the features which has received most attention is creep behaviour; however, this has been extensively considered only under stresses considerably lower than the yield stress. The data can be described by means of simple rules (constitutive equations or master curves), but only within very limited stress ranges[1–7].

The yield behaviour has also been extensively studied[8–11]. Several equations describing the effect of loading rate have been proposed[12–15].

Much less attention has been given to viscoelastic behaviour at very large strains (after yielding). In this zone, only qualitative information has been collected, and limited aspects have been analysed[15–17].

This work follows our previous paper[18] where tensile creep and stress–relaxation behaviour of Mylar after yielding were considered. A single master curve for the creep data was obtained independently of loading rate and stress level. The analysis of stress–relaxation tests was slightly less successful in as much as data relative to tests with the same initial stress could be collected into single curves independent of loading rate, while the dependence on initial stress was not completely accounted for.

Here, viscoelastic properties at large compressive deformations of a commercial polycarbonate are studied with the aim of obtaining master stress–relaxation and creep curves. As will be shown, simple criteria for superposition can be found. These criteria are very similar to those used for Mylar[18] in spite of the quite different physical structures (essentially amorphous *versus* semi-crystalline) and deformation modes (compression *versus* tension).

EXPERIMENTAL

The following compression tests were performed: constant velocity stress–strain, large deformation stress–relaxation and constant force creep. All data were obtained by an Instron testing machine operated, except when explicitly specified, at room temperature (about 20°C). For the creep tests, the strain was measured by a transducer system whose full scale sensitivity could be brought to one mm displacement.

The material used was Lexan, a bisphenol A polycarbonate (4,4′-dioxydiphenyl 2-2-propane carbonate; General Electric). Its average molecular weight, as determined by means of intrinsic viscosity measurements, was 25 000.

Data were taken at different loading rates and the deformation level for both the stress–relaxation and creep tests was brought up to about 70% reduction of the sample height.

All the samples had a cylindrical shape and were obtained by machining the supplied material in the form of a rod. Several exploratory tests were performed in order to investigate the influence of the sample shape. It was concluded that only the initial height/diameter ratio l_0/D_0 had a significant effect on the mechanical behaviour of the sample. If the height to diameter ratio is small[19], a constraint to the deformation is introduced by the friction between the dies and the sample; if the ratio is large, the sample becomes unstable and it buckles. However, it was observed that the mechanical behaviour of the sample is much less affected by the height/diameter ratio at very large deformations (after yielding) than it is at small deformations. By changing l_0/D_0 from 1 to 1.7, the stress–strain curves were reproducible to within 5% in the plastic region while the apparent initial modulus varied as much as 15%. Also stress–relaxation and creep data taken at 30% sample deformation were reproducible within 5% with a change of l_0/D_0 from 1 to 1.7.

All data reported in the following were obtained with cylindrical samples whose diameter and height were both 9 mm. They did not buckle (while buckling was observed for the samples of $l_0/D_0 = 1.7$) but deformed into a barrel shape, although this was not pronounced. In order to evaluate true stress–strain curves from load–sample height data, constant density was assumed and the barrelling was neglected.

0032–3861/80/040461–05$02.00

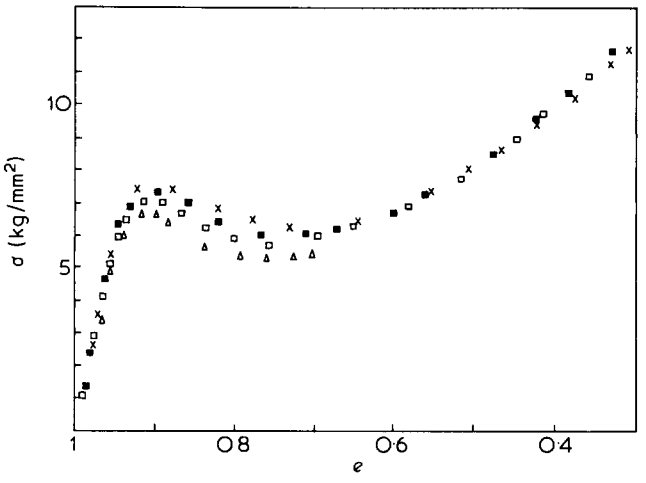

Figure 1 Compressive true stress σ *versus* strain e. α_0 is the initial deformation rate.

	α_0 (h^{-1})	T°C
□	3.3	20
■	33	20
x	132	20
△	3.3	45

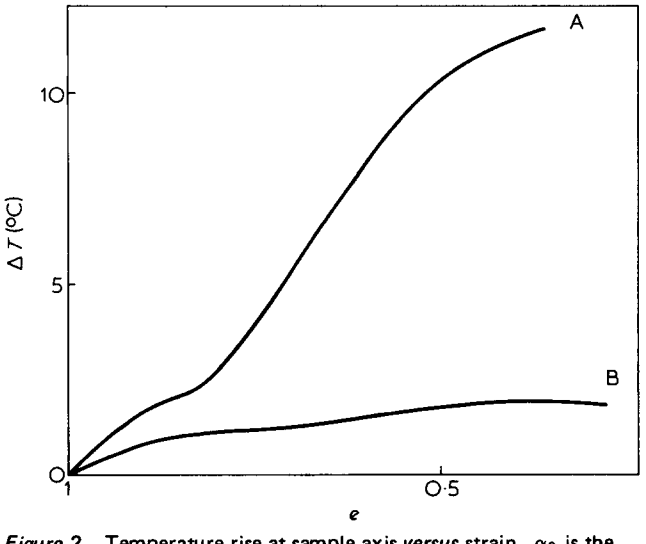

Figure 2 Temperature rise at sample axis *versus* strain. α_0 is the initial deformation rate. A, $\alpha_0 = 33\ h^{-1}$; B, $\alpha_0 = 3.3\ h^{-1}$

RESULTS

The true stress σ is plotted in *Figure 1 versus* the strain $e \equiv l/l_0$ (l is the current sample height and l_0 its initial value) in constant velocity compression tests. With this strain definition, larger deformations correspond to smaller strains. Three of the curves of this figure were obtained by deforming the material at room temperature (20°C) with different values of the initial deformation rate $\alpha_0 \equiv V/l_0$ where V is the velocity of the machine cross-head. These curves seem to show that after yielding the stress is independent of strain rate. Binder and Muller[20] have demonstrated that a considerable temperature rise may occur during large deformation compression tests. At sufficiently small values of the deformation rate, isothermal conditions can be achieved. The temperature rise at the sample axis was measured in order to detect whether the independence after yielding of stress on strain rate is to be ascribed to sample heating. The temperature rise, measured with the technique adopted by Binder and Miller[20], is plotted in *Figure 2 versus* the strain e. The data show that the temperature rise increases with deformation rate and that in the yielding zone it is relatively small for the larger deformation rate considered here. A remarkably larger temperature increase would be needed, as shown in *Figure 1*, in order to affect significantly the stress–strain behaviour in this zone.

Stress–relaxation tests have been made at different strains e_r produced by constant velocity strain ramps. The range of strains is from 0.91, which corresponds to yielding, down to 0.35 when the sample is very close to fracture. The loading rates were varied within a range smaller than that of the stress–strain tests. This was due to the fact that, at large velocities, the machine cross-head did not stop instantaneously but had a significant, albeit small, reverse motion. The data are plotted in *Figure 3* as σ/σ_0 *versus* the time t measured from the beginning of relaxation, when the stress is σ_0.

We now focus attention on stress–relaxation tests made after strain ramps performed with the same value of the initial deformation rate α_0. The data show that, as the sample deformation increases, (starting from yielding), the relaxation rate first increases, has a maximum in the strain zone where σ_0 has a minimum, and then decreases. At fixed values of α_0 and t, the values of the expression $1 - \sigma/\sigma_0$ are proportional to e_r, with the exception of the curves at e_r = 0.91 which relax more slowly. These curves (*Figure 1*) correspond to the maximum of stress during constant velocity tests. Their slow relaxation means that, at this strain level, the molecular structure is still rapidly changing with deformation towards an increase of molecular mobility. For a fixed strain e_r (0.91 included) the stress–relaxation curves strongly depend upon the initial deformation rate, α_0, of the loading ramp. In particular, analogous to that which was

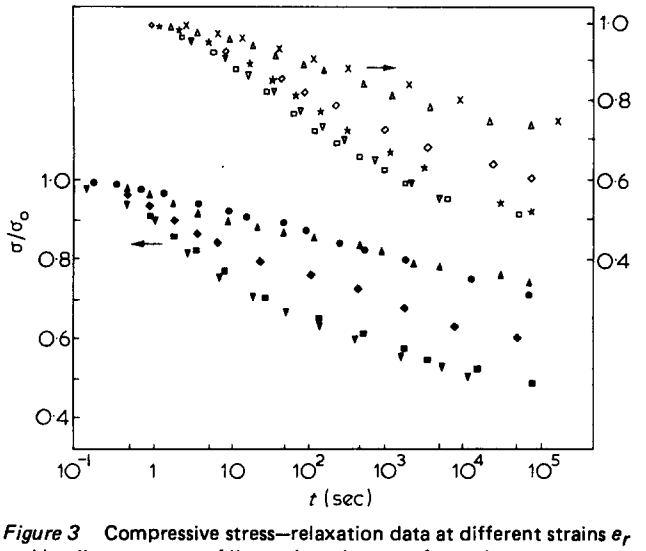

Figure 3 Compressive stress–relaxation data at different strains e_r and loading rates α_0. All tests have been performed at room temperature except ▽. (30°C)

α_0 (h^{-1})	33	3.3	1.65
e_r			
0.35	▲	△	
0.52	◆	◇	
0.70	■	□, ▽	
0.85	▼		*
0.91	●		x

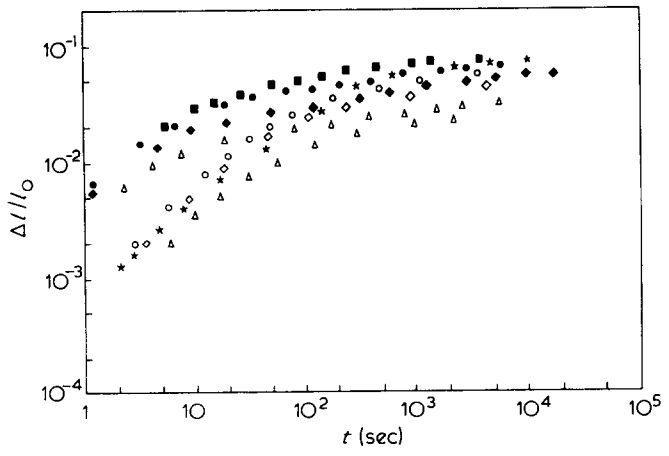

Figure 4 Compressive creep behaviour at different strains e_c and loading rates α_0.

	e_c		
	α_0 = 33 h^{-1}	α_0 = 3.3	α_0 = 1.65
0.7	■		*
0.63		○	
0.61	●		
0.50	◆	◇	
0.31	▲	△	

observed with Mylar[18], faster strain ramps generate larger relaxation rates. In order to separate the effect of the deformation rate from that of the heating along a stress–strain curve, a few particular stress–relaxation tests were performed. The data obtained during one of these are also shown in *Figure 3* and have to be compared with those collected under identical loading conditions (low loading rate and small temperature rise) at 20°C. Although a precise temperature is indicated in the figure, the experimental procedure adopted for this test was as follows: during the deformation, warm air (at about 30°C) was blown on the sample which was initially at 20°C. The air temperature was chosen so as to reproduce approximately, before the relaxation, the temperature rise observed with a deformation rate ten times larger. At the beginning of the relaxation, the warm air blow was interrupted and the sample was left to relax; during the relaxation the sample, similar to the case of heating due to deformation, was left to cool freely towards room temperature (20°C). The relaxation behaviour of this test (*Figure 3*) does not differ significantly from that of the corresponding test performed without a warm air blow, which did show a very small temperature rise.

This was assumed to demonstrate that the temperature changes which occurred before and during the stress–relaxation tests performed with the larger deformation rate do not alter the results significantly: the effect observed may be ascribed essentially to the deformation rate.

The creep tests were undertaken by deforming the sample with constant velocity strain ramps up to a fixed strain e_c and by holding a constant load thereafter. The data are plotted in *Figure 4* as $\Delta l/l_0$ *versus* t, where Δl is the displacement of the machine cross-head and t is time, both being measured from the end of the strain ramp. The behaviour observed is analogous to that shown by the stress–relaxation data. In fact, for tests made with the same initial deformation rate α_0 of the loading ramp, the creep deformation at a given time is smaller for smaller values of e_c, i.e. for larger initial deformations. Data taken at the same value of the initial strain e_c show that larger initial deformation rates α_0 produce faster rates of subsequent creep deformation. At small times, the creep strain $\Delta l/l_0$ is about proportional to α_0.

A few tests were performed in order to investigate the effect of the history of deformation on both creep and stress–relaxation behaviour. Instead of single constant velocity strain ramps, more complex loading modes were adopted. The same values of the initial strains e_r and e_c were reached by means of two consecutive strain ramps and, after the first ramp, the material was allowed stress-free recovery in many cases. Typical stress–strain curves obtained with these loading procedures are shown in *Figure 5*. When no recovery has taken place, increasing the velocity produces a secondary yielding process at the beginning of the second ramp. The details of the loading procedures are reported in *Table 1*. The data of the subsequent stress–relaxation or creep tests are plotted in *Figures 6* and *7*, respectively. The results of the corresponding 'normal' (single strain ramp) tests are plotted for comparison. Tests 5 and 6 (*Figure 6*) correspond to different loading histories but to the same values of both the strain e_r and the strain rate α_i just prior to the test: they showed the same relaxation behaviour. A similar comment holds for tests 7–10 and 10–13 considered in *Figure 6*. The effect of past loading history on creep behaviour is also negligible. This is shown in *Figure 7* where within each pair of tests 1–2 and 3–4, the same values of initial strain e_c and deformation rate α_i are retained but different loading procedures are considered. In conclusion, the viscoelastic behaviour at a given strain in the plastic region does not seem to depend on the complete loading history but only on the strain rate α_i in the last strain interval prior to the test. This statement must not be taken too literally because the strain rate of the second ramp in any test has been applied for a time long enough to approach the 'normal' stress–strain curve.

CREEP AND STRESS–RELAXATION MASTER CURVES

The time shift superposition principle was recently applied to tensile creep and stress–relaxation data taken at large

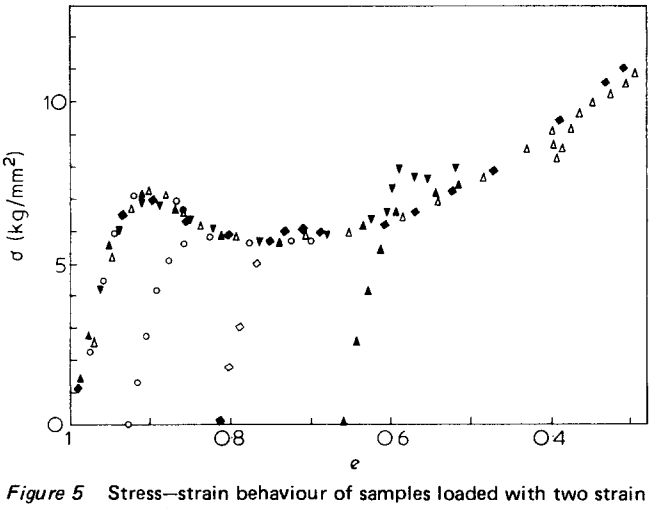

Figure 5 Stress–strain behaviour of samples loaded with two strain ramps. Details of loading procedures are given in *Table 1*. Test number: ○, 5; ▲, 8; ▼, 9; △, 12; ◆, 14

Table 1 Loading procedures of tests considered in *Figures 4–6*

Test type	Creep				Stress–relaxation									
Test number	1	2	3	4	5	6	7	8	9	10	11	12	13	14
Initial deformation rate of first ramp, h^{-1}	3.3	Single ramp	330	Single ramp	33	Single ramp	3.3	3.3	3.3	Single ramp	33	33	Single ramp	3.3
Strain achieved after first ramp	0.6		0.8		0.85		0.75	0.59	0.6		0.66	0.4		0.75
Free stress recovery	No		Yes		Yes		Yes	Yes	No		Yes	No		Yes
Deformation rate of second ramp with reference to l_0, h^{-1}	33	33	3.3	3.3	3.3	3.3	33	33	33	33	3.3	3.3	3.3	33
Initial strain of the test, e_c or e_r	0.5	0.5	0.31	0.31	0.7	0.7	0.5	0.5	0.5	0.5	0.31	0.31	0.35	0.3

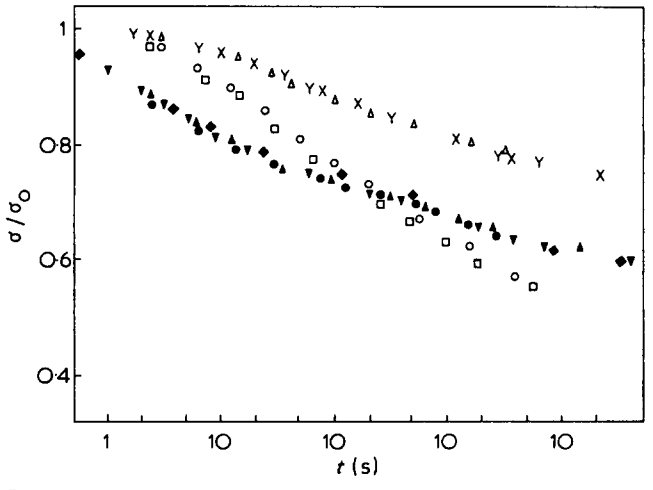

Figure 6 Stress–relaxation behaviour of samples loaded with two strain ramps. Details of loading procedures are given in *Table 1*. Test number: ○, 5; □, 6; ●, 7; ▲, 8; ▼, 9; ◆, 10; Y, 11; △, 12; X, 13

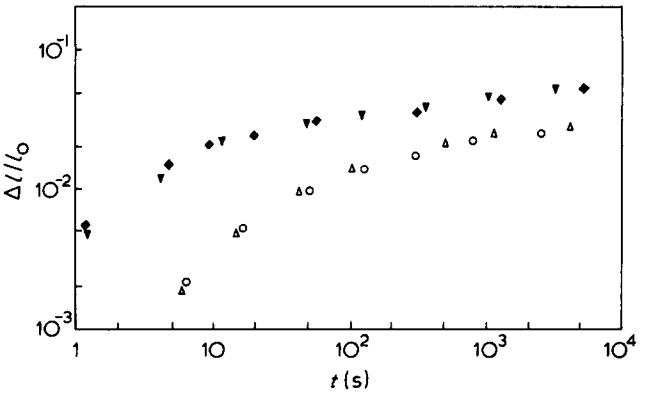

Figure 7 Creep behaviour of samples loaded with two strain ramps. Details of loading procedures are given in *Table 1*. Test number: ▼, 1; ◆, 2; ○, 3; △, 4

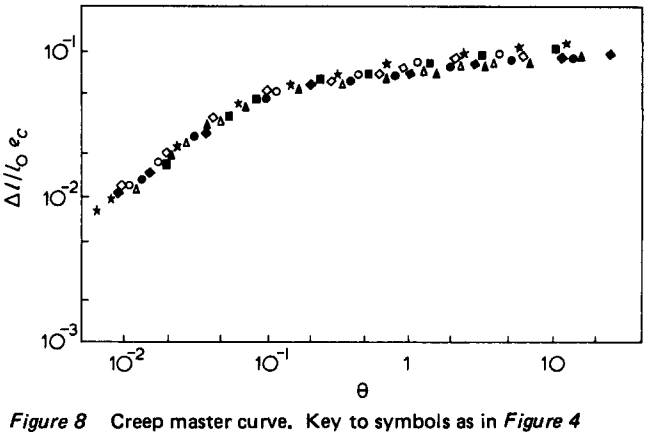

Figure 8 Creep master curve. Key to symbols as in *Figure 4*

deformations on Mylar samples[18]. Satisfactory results were obtained, especially for creep tests, by plotting the data as $\Delta l/l_0 e_c$ *versus* the dimensionless time $t \equiv t\alpha_i$. This normalization rule is equivalent to stating that, along a stress–strain curve, molecular mobility is a function only of the deformation rate and, in particular, that the material relaxation time changes proportionally to the inverse of α_i.

Similarly, the data presented in this paper show that at a given strain the initial values of both the stress–relaxation rate and the creep deformation are proportional essentially to the deformation rate. Consequently, for the material considered here, one can assume that the relaxation time τ changes proportionally to the inverse of α_i, *provided a constant value of the strain is considered.* A significant difference from the previous data[18] is that the influence of deformation cannot be ignored in the results presented here. The structural modifications concomitant with plastic deformation change molecular mobility; the data in *Figure 4* show that the relaxation time τ (one should really talk about a spectrum of relaxation times) is a decreasing function of deformation. In a following section we shall consider the influence of deformation in greater detail to show that the observed differences between the results presented here and those previously reported[18] can be reconciled.

To account for the influence of deformation on relaxation time, we assume here the simple expression:

$$\tau \propto 1/(e\alpha_i) \qquad (1)$$

which is used for the time shift procedure. This assumption was suggested mainly by the fact that at a constant value of the deformation rate α_i, for deformation larger than the yield deformation, the initial relaxation rate (and thus the inverse of the relaxation time) and the strain e both decrease as the compressive deformation proceeds.

Figure 8 shows that a single master curve is obtained by plotting all creep data of *Figure 4* as $\Delta l/l_0 e_c$ *versus* the dimensionless time:

$$\theta = te_c\alpha_i \propto t/\tau \qquad (2)$$

The same dimensionless time, except for the obvious substitution of e_r for e_c in equation (2), is used in *Figure 9*

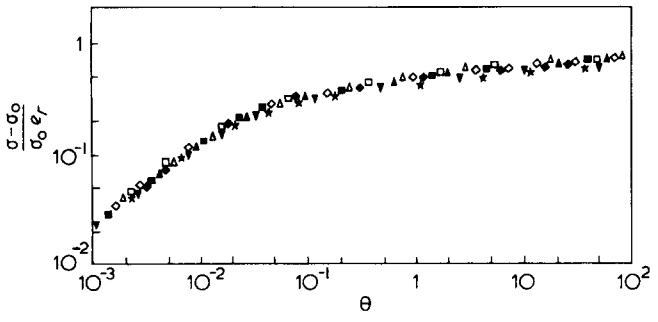

Figure 9 Stress–relaxation master curve. Key to symbols as in *Figure 3*

for the stress–relation data. For these data, however, a somewhat more detailed analysis is required in order to determine the appropriate dimensionless stress measure. As already observed[18,21,22], one should consider the 'relaxable' stress, i.e. $\sigma - \sigma_\infty$, where σ_∞ is the stress value asymptotically approached after a sufficiently long time. The ratio $(\sigma - \sigma_\infty)/(\sigma_0 - \sigma_\infty)$ would be an appropriate dimensionless stress. Unfortunately the value of σ_∞ cannot be measured directly, but this difficulty can be circumvented by the following argument. In the previous section, it was observed that, for fixed values of α_i and t, the quantity $1 - \sigma/\sigma_0$ is proportional to the initial strain e_r. By assuming that this proportionality holds after an infinite time, one writes:

$$1 - \sigma_\infty/\sigma_0 = Ae_r \tag{3}$$

where A is a constant. Thus the dimensionless relaxable stress can be written as:

$$\frac{\sigma - \sigma_\infty}{\sigma_0 - \sigma_\infty} = 1 - \frac{\sigma_0 - \sigma}{A\sigma_0 e_r} \tag{4}$$

Equation (4) shows that, if the group on the left hand side is a function of θ only, the same property must be shared by the group $(\sigma_0 - \sigma)/\sigma_0 e_r$ which can be easily obtained from the data. *Figure 9* shows a satisfactory superposition of the stress–relaxation results in terms of the above mentioned group and dimensionless time θ.

Should the superposition rules, adopted in *Figures 8* and *9*, be verified by different polymers, a single creep or relaxation test would be sufficient to specify the creep or relaxation behaviour (in compression) after yielding for any loading history and any strain level.

FURTHER COMMENTS ON THE INFLUENCE OF DEFORMATION

The tensile stress–relaxation data for Mylar[18] show that σ_∞/σ_0 increases, although rather weakly, with sample elongation and thus with $e_r = l/l_0$. In an effort to find an expression for σ_∞/σ_0 which is satisfied both in the case examined in this work and in tensile stress–relaxation tests, one should substitute for e_r in equation (3) a strain measure which in compression is approximately equivalent to e_r, while in tension it becomes a weak decreasing function of e_r. The square root of the second invariant of the inverse of the Cauchy tensor[23], **C**, evaluated with reference to the virgin unoriented material configuration, is dominated by l_0/l when this is larger than one, i.e. in compression; and grows more slowly than l/l_0 when l_0/l is smaller than one, i.e. in tensile tests. A possible generalization of equations (2) and (3) can thus be obtained by substituting e_r and e_c by the inverse of $\sqrt{II_{C-1}}$. The influence of the correction term $\sqrt{II_{C-1}}$ is sufficient to account for the observed differences as far as the stress–relaxation data previously reported[18] are concerned and it is sufficiently weak to maintain a good superposition between the creep data reported there. This suggestion should be checked with other materials and with the same material in tension and compression.

ACKNOWLEDGEMENT

This work has been supported by C. N. R. Grants 77.00624.03 and 78.00935.03. Thanks are due to Mr. G. A. Troia for machining the samples.

REFERENCES

1 Findley, W. N. and Khosla, G. *J. Appl. Phys.* 1955, **26**, 821
2 Passaglia, E. and Koppehele, H. E. *J. Polym. Sci.* 1958, **33**, 281
3 Turner, S. *Br. Plast.* 1965, 44; *ibidem* 1965, 106
4 Hall, I. H. *J. Polym. Sci.* A-2, 1967, **5**, 1119
5 Ward, I. M. and Wolfe, J. M. *J. Mech. Phys. Solids*, 1966, **14**, 131
6 Morgan, C. J. and Ward, I. M. *J. Mech. Phys. Solids*, 1971, **19**, 165
7 Yannas, I. V. *J. Polym. Sci.* 1974, **9**, 163
8 Bauwens, P. B. and Raha, S. *Phil. Mag.* 1970, **22**, 463
9 Holt, D. L. *J. Appl. Polym. Sci.* 1968, **12**, 1653
10 Duckett, R. A., Rabinowitz, S. and Ward, I. M. *J. Mat. Sci.* 1970, **5**, 909
11 Bauwens, J. C., Bauwens-Crowet, C. and Holmes, G. *J. Polym. Sci. A-2*, 1969, **7**, 1745
12 Brady, T. E. and Yeh, G. S. Y. *J. Appl. Phys.* 1971, **42**, 4622
13 Ree, T. and Eyring, H. *J. Appl. Phys.* 1955, **26**, 793
14 Robertson, R. E. *App. Polym. Symp.* 1968, **7**, 201
15 Kramer, E. J. *J. Appl. Phys.* 1970, **41**, 4327
16 Kramer, E. J. *J. Appl. Polym. Sci.* 1970, **14**, 2825
17 Richards, R. C. and Kramer, E. J. *J. Macromol. Sci. Phys. B.* 1972, **6**, 229
18 Titomanlio, G. and Rizzo, G. *J. Appl. Polym. Sci.* 1977, **21**, 2933
19 Haward, R. N. 'The physics of glassy polymers', Applied Science, London, 1973
20 Binder, G. and Muller, F. H. *Kolloid. Z.* 1961, **177**, 129
21 Kubat, J., Petermann, J. and Rigdahl, M. *Mat. Sci. Eng.* 1975, **19**, 185
22 Kubat, J., Petermann, J. and Rigdahl, M. *J. Mat. Sci.* 1975, **10**, 2071
23 Astarita, G. and Marrucci, G. 'Principles of non-Newtonian fluid mechanics', McGraw-Hill, London, 1974